

Curcumin-1,2,3-Triazole Conjugation for Targeting the Cancer Apoptosis Machinery

Francesca Seghetti^{1^}, Rita Maria Concetta Di Martino^{1^§}, Elena Catanzaro^{2^}, Alessandra Bisi¹, Silvia Gobbi¹, Angela Rampa¹, Barbara Canonico³, Mariele Montanari³, Dmitri V. Krysko⁴, Stefano Papa³, Carmela Fimognari^{2*} and Federica Belluti^{1*}

¹ Department of Pharmacy and Biotechnology, Alma Mater Studiorum-University of Bologna, Via Belmeloro 6, 40126 Bologna, Italy; [§]Present address: Department of Drug Discovery and Development, Istituto Italiano di Tecnologia, via Morego n.30, 16163 Genova, Italy.

² Department for Life Quality Studies, Alma Mater Studiorum-University of Bologna, Corso d'Augusto 237, 47921 Rimini, Italy.

³ Department of Biomolecular Sciences, University of Urbino Carlo Bo, Urbino, Italy.

⁴ Cell Death Investigation and Therapy Laboratory, Department of Human Structure and Repair, Ghent University, Ghent, Belgium; Cancer Research Institute Ghent, Ghent, Belgium; Department of Pathophysiology, Sechenov First Moscow State Medical University, Moscow, Russia.

[^]These authors contributed equally to this work.

* Correspondence: federica.belluti@unibo.it; Tel.:+39 0512099732 (FB) + carmela.fimognari@unibo.it; Tel.:+390541-434-658 (CF)

1. Structural Characterization of Compound 1.

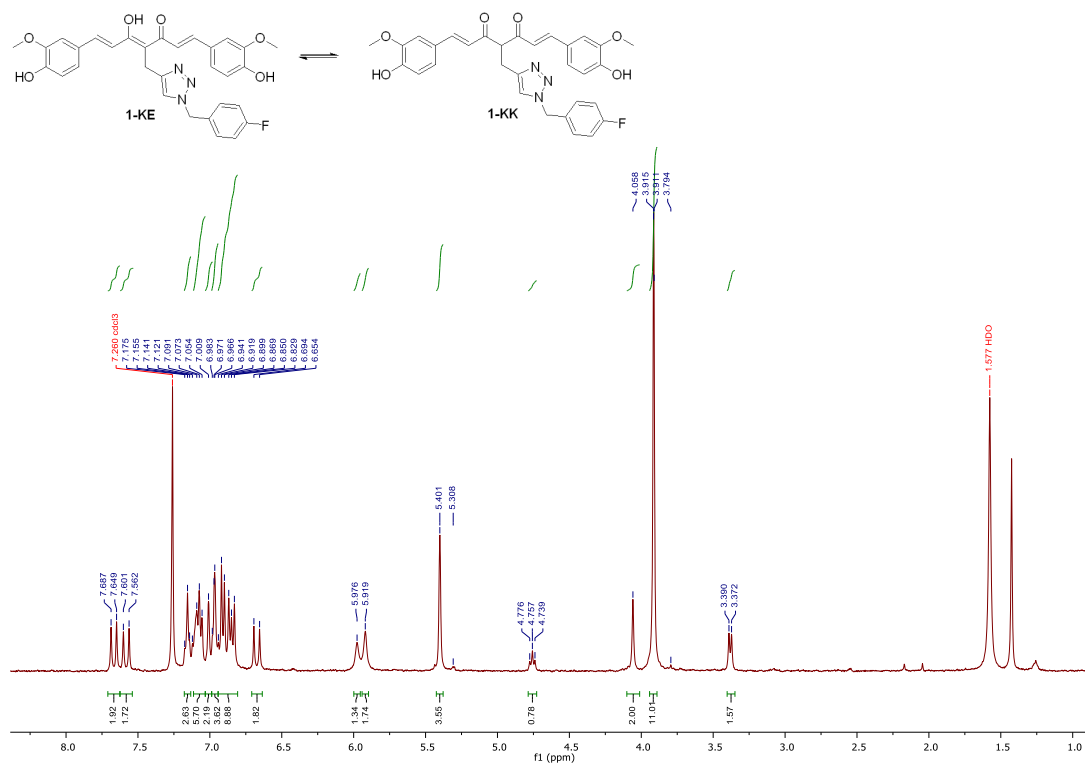


Figure S1. ¹H NMR (CDCl₃, 400 MHz) copy of compound 1.

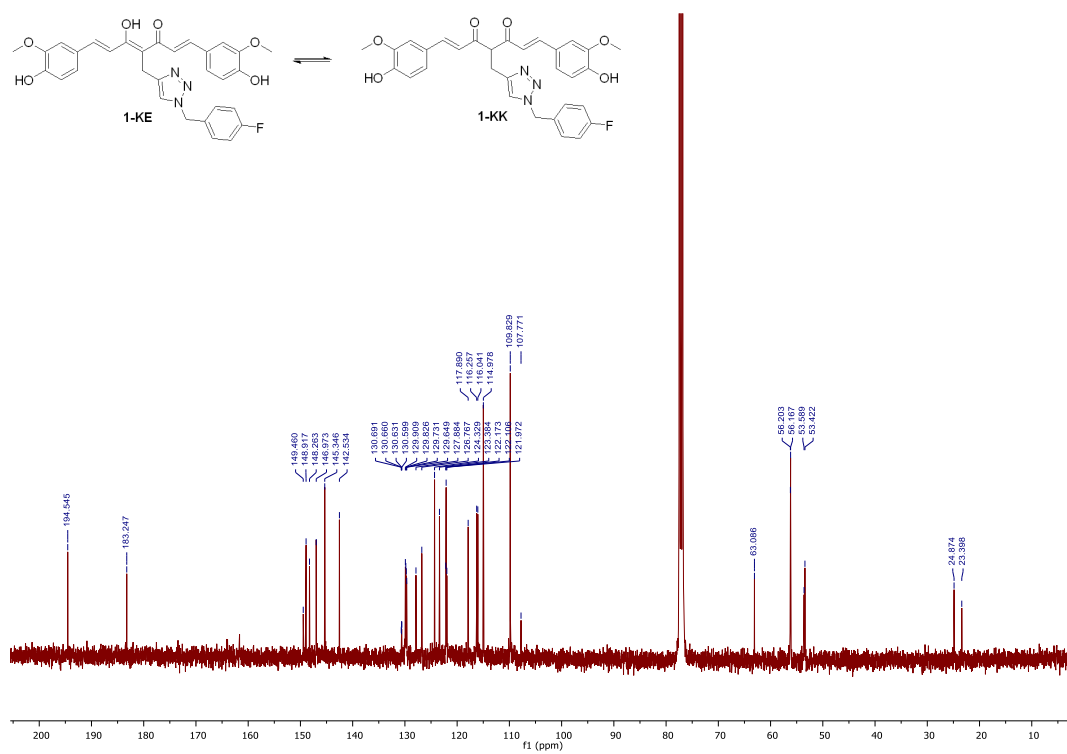


Figure S2. ^{13}C NMR (CDCl₃, 101 MHz) copy of compound 1.

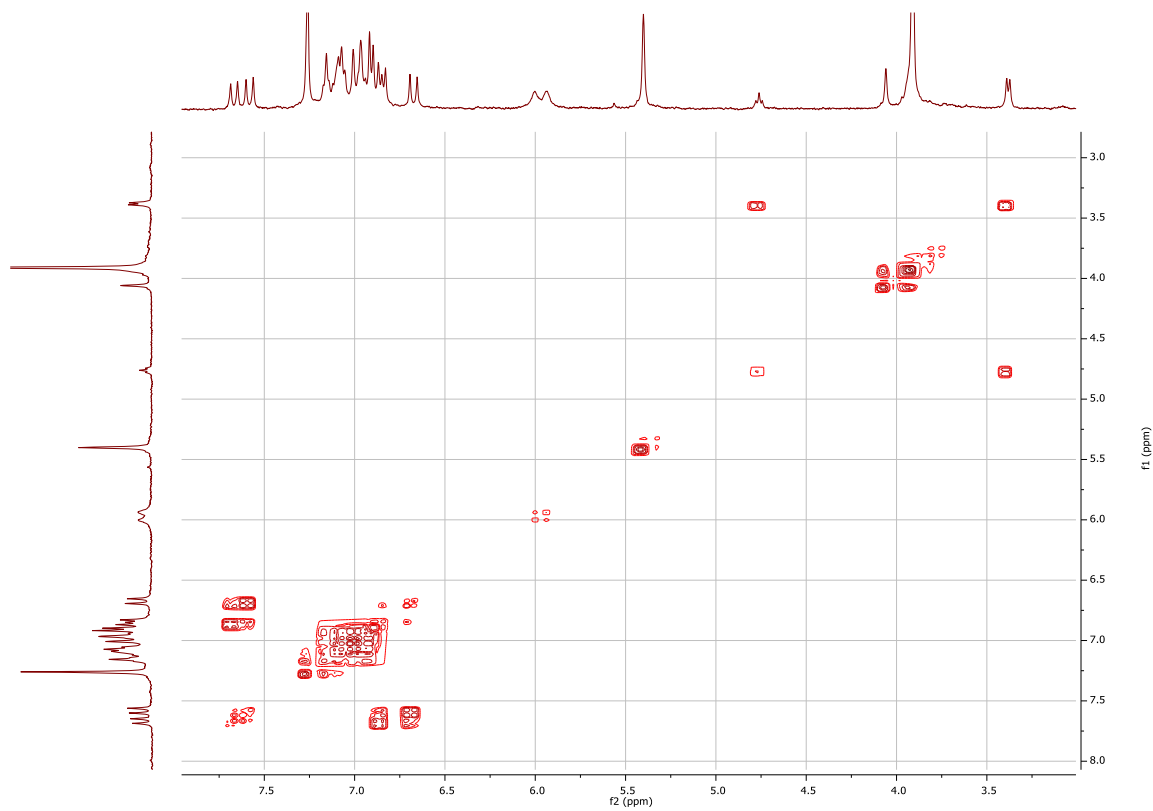


Figure S3. ^1H - ^1H COSY copy of compound 1.

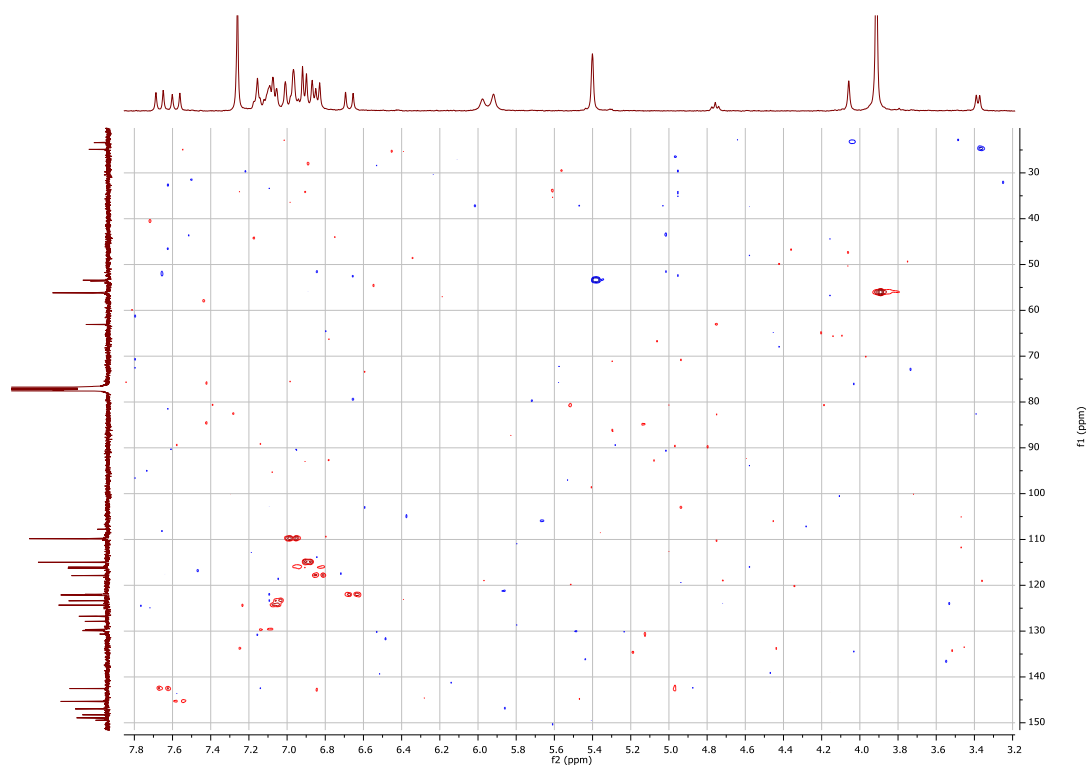


Figure S4. ^1H - ^{13}C HSQC copy of compound 1.

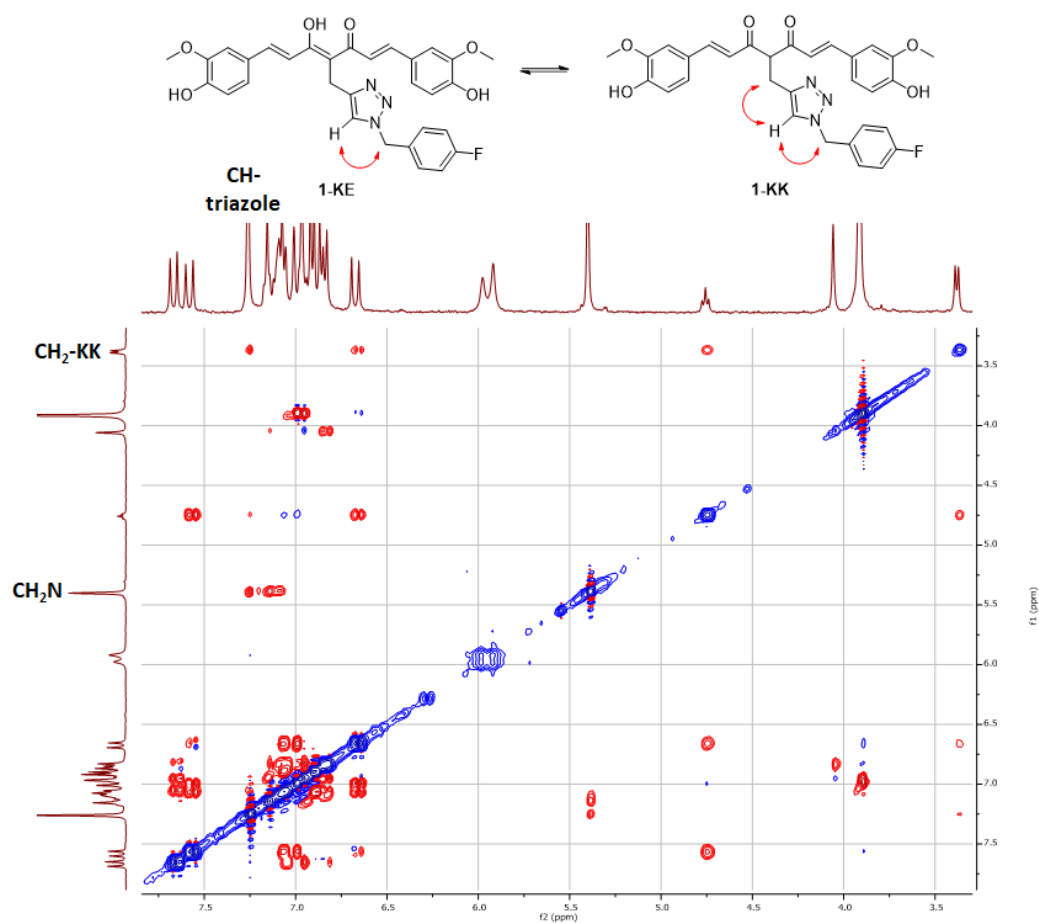


Figure S5. 2D NOESY copy of compound 1.

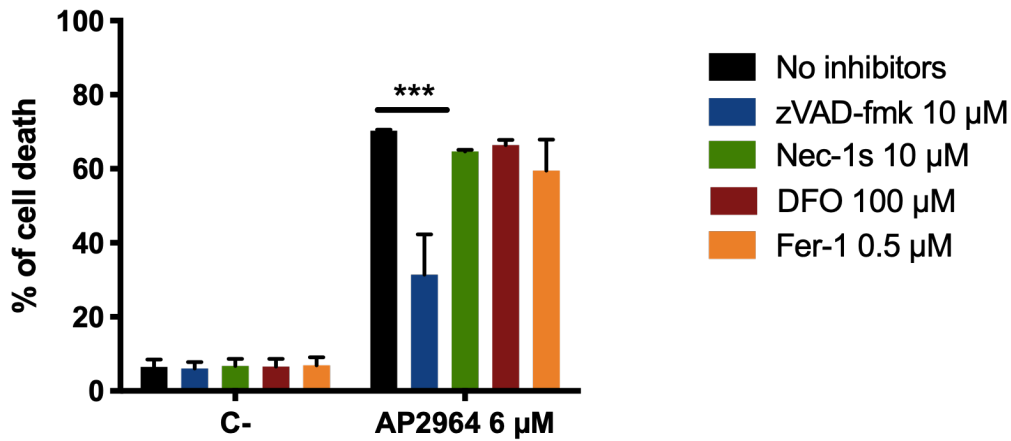


Figure S6. Cell-death analysis of Jurkat cells (% of dead cells) pre-treated for 1h with zVAD-fmk, Nec-1s, DFO, or Fer-1 and then treated with compound 1 for 48h. *** P < 0.001.

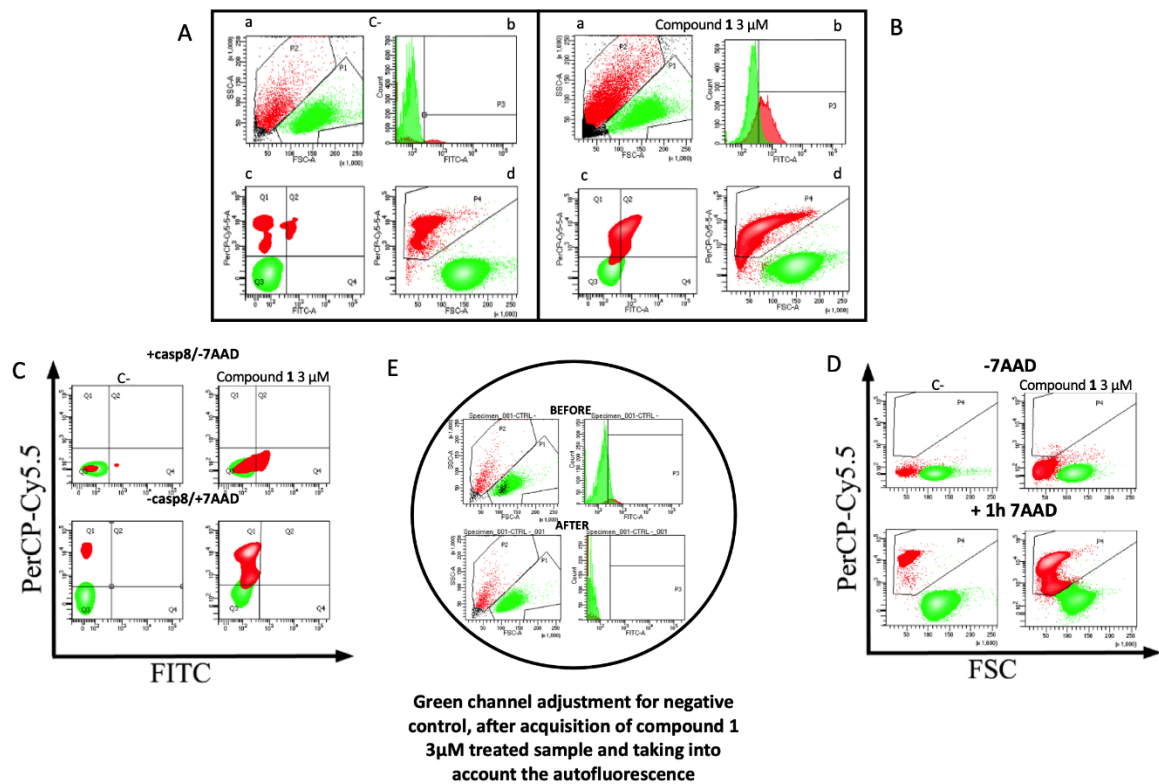


Figure S7. Gating strategy (A, B, C, D) and green autofluorescence management (E) in caspase 8 analysis. (A) and (B) show the sequence of dot plots, histograms and contour plot of control and compound 1-treated samples, respectively. CCRF-CEM were split into different sub-populations depending on the morphologic parameters: red gate shows dead cells, green gate shows viable cells. Black represents debris which were excluded for the analysis. Dot plots in the picture show control (Aa) untreated cells and cells treated with the compound 1 for 24 h (Ba). In particular, (Ba), highlights the huge increase of red events, *i.e.* shrunken virtually apoptotic cells. To clear identify the apoptotic process, 7-AAD and Caspase 8 labelling were performed: histograms (Ab) and (Bb) show caspase 8 positivity (very low in control cells, while relevant in compound 1-3 μM-treated cells); contemporary contour plots (Ac) and (Bc) highlights caspase 8+/7-AAD+ cells. Finally, the

contour plot FSC vs PerCpCy5.5 demonstrates how 60 minutes of incubation at RT for 7-AAD well discriminate between apoptotic (7-AAD^{low}) and necrotic-or late apoptotic (7-AAD^{bright}) cells. Since compound **1** emits fluorescence, the test required several steps and checkpoints, however it was possible to perform it. In (C), contour plots FITC vs PerCpCy5.5 are shown for control and compound **1**-treated samples: the first-row highlights both samples only for caspase 8 labelling, the second row only for 7-AAD uptake. Furthermore, (D) underlines, for control and compound **1**-treated samples, the positioning of the area of 7-AAD positivity (for both 7AAD^{low} and 7AAD^{bright} events), taking into account distribution of events in unlabeled samples (the upper row). Finally, in (E), as stated in the figure, the step of green channel adjustment.

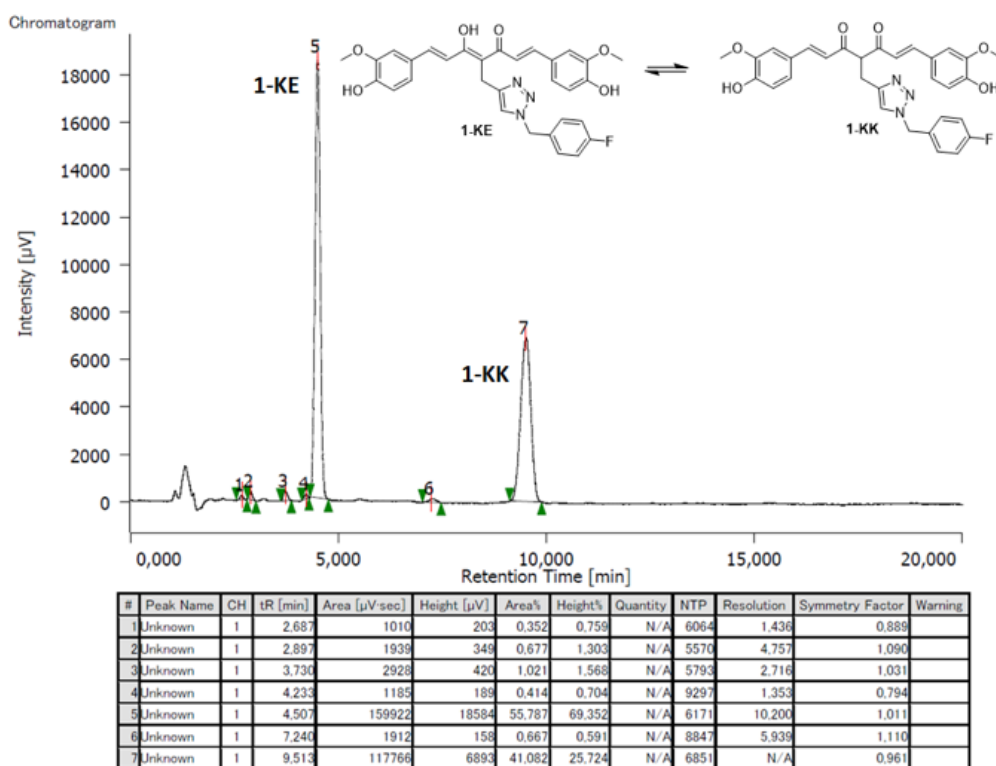


Figure S8. HPLC copy for compound **1**.

Physicochemical Properties Prediction. The online server FAFDrugs4 (server available at <http://fafdrugs4.mti.univ-paris-diderot.fr>) was used to predict physicochemical properties of compounds **1-6**, including logP, logD (at pH 7), flexibility, aqueous solubility (logSw), number of rotatable bonds, hydrogen-bond acceptors (HBAs), and hydrogen-bond donors (HBDs). FAFDrugs4 was also applied to predict the filter PAINS elements among compounds **1-6**. The screening was performed using all three available PAINS filters (PAINS filter A, B and C). None of the screened target compounds contained a PAINS substructure.

Table S1. Physicochemical properties prediction for compounds **1-6**

	logP	logD	logSw	RotatableB	RigidB	Flexibility	HBD	HBA	HBD_HBA
1	5.41	5.37	-6.23	11	27	0.29	3	9	12
2	5.28	5.08	-6.14	12	27	0.31	3	10	13
3	5.33	5.68	-6.0	11	27	0.29	2	8	10
4	5.2	5.38	-5.92	12	27	0.31	2	9	11
5	6.67	7.74	-7.61	15	38	0.28	1	10	11

6	6.41	7.14	-7.44	17	38	0.31	1	12	13
---	------	------	-------	----	----	------	---	----	----

Table 2. Physicochemical properties prediction for compounds 1-6

ù	Rin gs	MaxSize Ring	NumCha rges	TotalCh arge	HeavyAt oms	CarbonAt oms	HeteroAt oms	ratio H/C	LipinskiViol ation
1	4	6	0	0	41	31	10	0.32	2
2	4	6	0	0	42	32	10	0.31	2
3	4	6	0	0	39	30	9	0.30	2
4	4	6	0	0	40	31	9	0.29	2
5	6	6	0	0	51	39	12	0.31	2
6	6	6	0	0	53	41	12	0.29	3

Table S3. PAINS filters for compounds 1-6

	Solubility ForecastIn dex	Oral Bioavaila bility VEBER	Oral Bioavaila bility EGAN	Phospholip idosis	Fsp3	PAIN S Filter A	PAIN S Filter B	PAIN S Filter C	Result
1	Reduced Solubility	Low	Low	NonInduce r	0.13	0	0	0	Accepted
2	Reduced Solubility	Low	Low	NonInduce r	0.16	0	0	0	Accepted
3	Reduced Solubility	Good	Good	NonInduce r	0.10	0	0	0	Accepted
4	Reduced Solubility	Good	Good	NonInduce r	0.13	0	0	0	Accepted
5	Reduced Solubility	Good	Good	NonInduce r	0.10	0	0	0	Accepted
6	Reduced Solubility	Low	Low	NonInduce r	0.15	0	0	0	Accepted